

Short Communication

In Situ Synthesis of Nanosized NiO Encapsulated in Graphene as High-performance Supercapacitor Cathode

Danfeng Qiu^{1,*}, Xiao Ma¹, Jingdong Zhang¹, Zixia Lin² and Bin Zhao²

¹Key Laboratory of Radar Imaging and Microwave Photonics (Nanjing Univ. Aeronaut. Astronaut.), Ministry of Education, College of Electronic and Information Engineering, Nanjing University of Aeronautics and Astronautics, Nanjing, 210016, China

²National Laboratory of Microstructures and School of Electronic Science and Engineering, Nanjing University, Nanjing, China

*E-mail: dfqiu@nuaa.edu.cn

Received: 13 May 2018 / Accepted: 2 July 2018 / Published: 5 August 2018

NiO nanoparticles embedded in graphene nanosheets (GNS) were successfully prepared by coprecipitation and pyrolysis beforehand. The three-dimensional GNS matrix with interconnected pore network structure can be filled with electrolyte ions serving as a double ion buffer pool during charge and discharge. High conductivity graphene, as a three-dimensional network, can be used to support the fast transmission of charge inside the NiO electrode during charging and discharging processes and meanwhile increase the performance rate. Hence, the NiO/GNS nanocomposites exhibit specific capacitance value of 1125.8 F g⁻¹ at a current density of 2 A g⁻¹ in 2 M KOH solution. This composite exhibits a good cyclic stability, with a small loss of 5.2% of maximum capacitance over a consecutive 2000 cycles, indicating that the prepared NiO/GNS nanocomposites serve as potential and promising candidates for supercapacitor electrodes.

Keywords: Graphene; Nickel oxide; Nanocomposites; Energy storage and conversion; Supercapacitors

1. INTRODUCTION

Supercapacitors have promising prospects in terms of their application in the field of electric vehicle power supply, portable electronics and various of high power industry equipment because of its high output power and long life [1-5]. However, it is found that supercapacitor has comparatively lower energy density than that of the battery, which requires people need to increase the energy density without sacrificing the power density and life of the capacitors. To realize this, there were various

means being used. By the nanocrystallization of electrode materials, the contact area between electrodes and electrolytes can be enlarged, which is one of the most commonly used means of increasing the capacity of supercapacitors[6-8]. The double layer capacitance produced by charge separation is a mechanism related to the specific capacitance of supercapacitors. The typical material of the double layer capacitance material is the classic material of activated carbon and carbon fiber, carbon nanotube and graphene, enjoying the advantages of high specific surface area and long cycling life stability. Another mechanism is pseudopotential behavior derived from reversible Faraday reaction[9-11]. While the electrode materials of pseudocapacitor, use of transition metal materials metal oxides, such as Co_3O_4 [12], RuO_2 [13], MnO_2 [14] and NiO [15] etc, has been intensively researched and hence to improve the capacity of electrodes according to their reversible oxidation-reduction reaction. Among all kinds of transition metal oxides, NiO has been attached with great attention due to its high theoretical specific capacity, abundant reserves and non-toxic properties[16-19]. However, the conductivity of NiO electrode material is relatively low. Therefore, it would be difficult to use it at the charging and discharging processes.

To address these challenges, various methods, such as preparation of nanoscale electrode materials, hybridization with carbonaceous materials, and adulteration of foreign atoms, are provided for the preparation of nano NiO electrode materials [20-22]. As a typical strategy, nano scale NiO electrode materials such as nanosheets, nanoparticles and nanowires can be used to expand the surface area of active electrodes. However, there are some issues remained to be solved, such as the poor cycling performance, limited electrical active point and inherent low conductivity of nano NiO materials [23]. In order to solve these problems, a strategy can be adopted, which is to hybridize with carbonaceous materials, such as amorphous carbon, carbon nanotubes and graphene [24], which can improve electrical conductivity and structural stability of the electrodes.

As a two-dimensional material, graphene is widely used as a carrier of active materials for various electrochemical devices because of its high specific surface area and electrical conductivity. The application of graphene loaded NiO as a supercapacitor electrode, graphene can give NiO physical support during charging and discharging processes due to its stable physical and chemical properties. Meanwhile, the graphene itself has the capacity of pseudopotential. The strong conductivity of graphene enables the charge in the NiO electrode material to be rapidly transported through the graphene network to the electrode and hence to realize fast charge and discharge.

In our study, we used a three-dimensional interconnected graphene array as a carrier while NiO nanoparticles were in situ grown in graphene matrix by one-step method as electrode materials for supercapacitors. Compared with other deposition technologies, it enjoys advantages of suitable for mass production, rapid production, simple installation and low cost.

2. EXPERIMENTAL

The natural graphite powders (universal grade, 99.985%) are used for the synthesis of graphite oxides (GOs) based on a modified Hummers method [25]. The graphite oxides need to be prepared beforehand, being exfoliated at 300 °C for 3 min in air. Afterwards, the graphite oxides need to be

treated under 900 °C for 3 h in Ar. The graphene nanosheets (GNS) is formed [26]. During the typical synthesis course of the nanocomposites of NiO/GNS, 581.6 mg of $\text{Ni}(\text{NO}_3)_2 \cdot 6\text{H}_2\text{O}$ was mixed with 50 mL of ethanol. A 50 mg portion of as-prepared GNS was put into the solution. Afterwards, it was treated ultrasonically for 5 min. A magnetic stirrer was mixed with the suspension in the ventilation cabinet before the evaporation of ethanol in solution.

Then, it collected the dried $\text{Ni}(\text{NO}_3)_2 \cdot 6\text{H}_2\text{O}$ /GNS composites at 200 °C for 10 h in air. $\text{Ni}(\text{NO}_3)_2 \cdot 6\text{H}_2\text{O}$ was then changed into NiO nanoparticles. The related mechanism is presented in below:



There was 75% of the NiO content in NiO/GNS in terms of weight. The $\text{Ni}(\text{NO}_3)_2 \cdot 6\text{H}_2\text{O}$ was heated under 200 °C for 10h in air to get the NiO sample ready for the control experiment. The base materials (9 wt.%) like N,N di-methyl-acetamide (~10 ml) and PVDF (1 wt.%) were mixed with a binder to fabricate NiO/GNS. Then, it stirred the final mixture for approximately 24 h in a magnetic stirrer (1200 rpm) under the room temperature. Subsequently, a thin graphite-sheet was used to cover the final product (specific area of $1 \times 1 \text{ cm}^2$). Then, the electrodes needed to be dried under 60°C for about 3 h in hot air oven. It has been found that the mass loading of the active materials over the graphite sheet is around $1.2 \text{ mg} \cdot \text{cm}^{-2}$ for electrodes being fabricated. During the control experiment, it also prepared pure NiO and pure GNS nanoplates (average size, 100 nm) through the same Electrochemical active materials/binder ratio (90:10). The supercapacitor electrodes are used to make accurate comparison with electrochemical properties of the resultant electrodes.

A three-electrode system was used to perform the electrochemical measurements, for instance pure NiO and NiO/GNS (working electrode), platinum wire (counter electrode) and saturated calomel electrode (reference electrode). The working electrode was conducted under 2 M KOH. Electrochemical workstation (CH1660C) was used for the analysis. The galvanostatic charge-discharge and cyclic voltammetry (CV) techniques were adopted to study the electrochemical behavior of the samples. The electrochemical features of pure NiO nanoplates and GNS were explored for the report and comparison.

3. RESULTS AND DISCUSSION

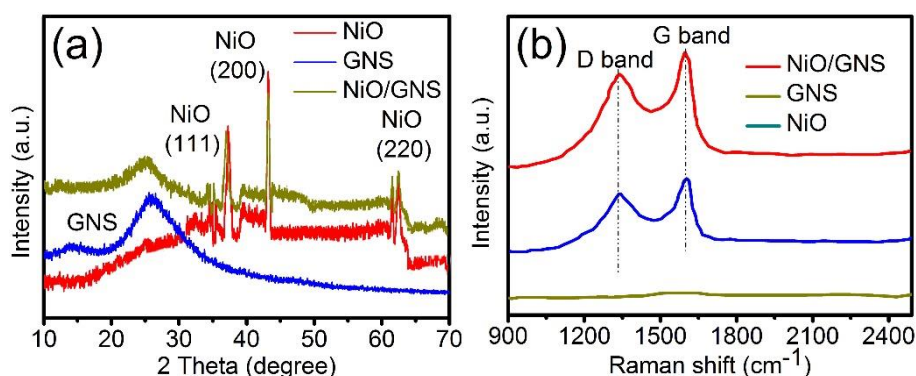


Figure 1 .(a) XRD and b) Raman characterizations of NiO and NiO/GNS samples.

The X-ray diffraction (XRD) and Raman are the features of pure NiO and NiO/GNS nanocomposites. As demonstrated in Figure 2a, the peaks of all the samples appeared under 37.2° , 43.2° , and 62.8° , which were correspondingly indexed to the (111), (200), and (220). The standard data (JCPDS file number 40-1467) provided NiO. The diffraction peak of the multilayer graphene of the GNS sample appeared under 25° . It has been demonstrated from Figure 2b the two sharp peaks occurred on 1345 and 1575 cm^{-1} , according to the disorder induced by D band and graphitic G band. The high crystallinity nature of the graphene layers of the NiO/GNS composites was demonstrated by the sharp and high G band.

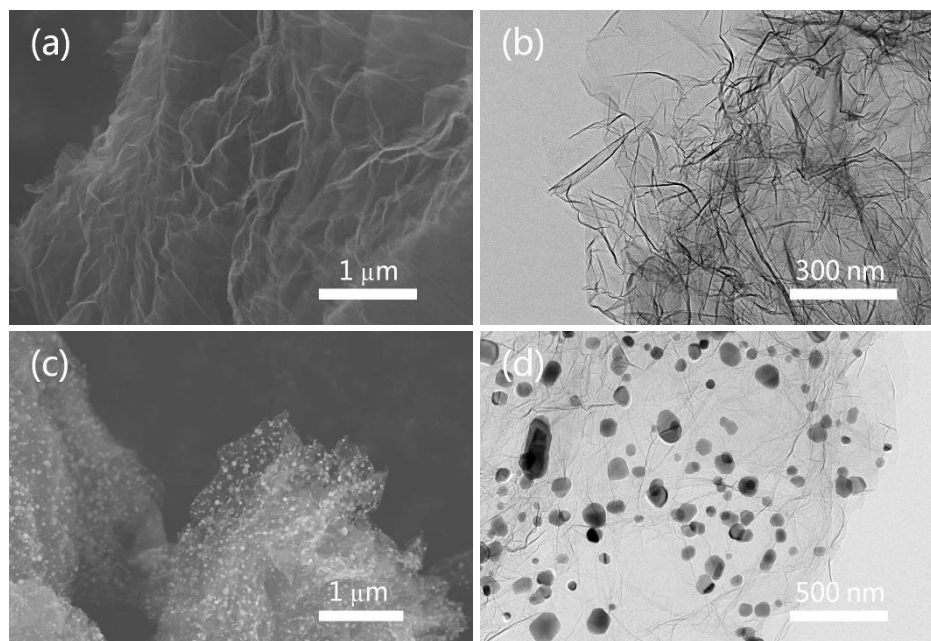


Figure 2. SEM (a) and TEM (b) images of mesoporous NiO nanoplates; SEM (c) and TEM (d) images of GNS; SEM (e) and TEM (f) images of NiO/GNS.

The SEM and TEM images of the GNS are shown in Figures 2a and 2b. The nanoscale structures are shown by the GNS samples. This is because of the decomposition of oxygen groups of GOs in the process of thermal exfoliation. Figures 2c and 2d demonstrated a classical scanning electron microscopy (SEM) and transmission electron microscopy (TEM) images of the NiO/GNS nanocomposites. The diameters of NiO nanoparticles are between 30nm and 100nm, which are closely integrated with GNS matrix. Meanwhile, they were also distributed along the GNS matrix homogeneously.

A pair of reversible redox peaks in 0.1-0.45 V was demonstrated by the CVs of all electrodes in figure 3a. The faradic conversions among various Ni species of alkali medium were triggered because of this. There was an increase of the scan rate from 5 and 100 mV/s. This suggests that NiO/GNS has strongly reversible redox reaction. Such electrode might lead to fast redox reactions for electrochemical energy storage due to the transport of faster electron and transfer of kinetics. Profiles of NiO/GNS electrode, including the galvanostatic charge/discharge under different current densities from 2 to 50 A g^{-1} are shown in Figure 3b. Figure 3c displays the differences of the specific

capacitance of various electrode materials having different densities from 2 to 50 A g⁻¹. It was found that NiO/GNS composites have the highest specific capacitance of all the samples. It needs to be pointed out that the composites are delivered in an excellent rate capability.

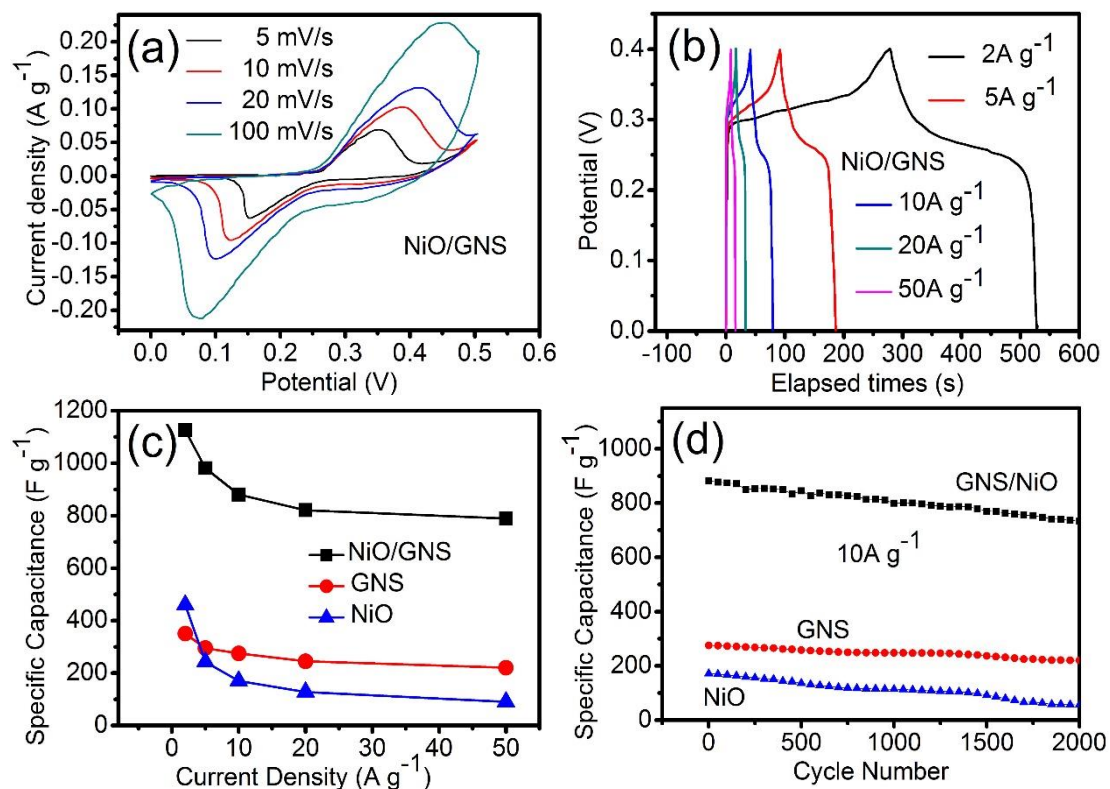


Figure 3. (a) CV curves of NiO/GNS with different scan rates; (b) charge/discharge curves of NiO/GNS at various current densities; (c) the specific capacitance of composites with different current densities; (d) cycling performances of composites at current density of 10 mA g⁻¹.

There was an increase of the current density from 2 to 50 A g⁻¹. NiO/GNS composites have 70.2% capacitance retention rate, which is way larger compared with pure NiO (20.1%). The majority of other reported NiO-based electrodes are superior to some advanced carbon materials for high-rate supercapacitor. The reason can be illustrated through the high electrical conductivity of the ultrafine NiO nanoparticles and the graphene sheets. More importantly, the oxygen vacancies over the mesoporous NiO nanoparticles of the graphene matrix is of great importance for the enhancement of the rate capability. Fig. 3d showed the cycleabilities of various electrodes at 10 A g⁻¹. The initial capacitance maintaining ratios of NiO/GNS, GNS and NiO electrodes were 83, 80 and 31%, respectively after 2000 repeated galvanostatic charge-discharge (GCD) curves. It has been found that NiO/GNS electrode decreased slowest because of the close connection with flexible graphenes. NiO/GNS nanocomposites are taken as the ideal faradic electrode material due to the strong cycle ability and rate capability and also the lowest self-discharge characteristic [27, 28].

As compared with other types of NiO based supercapacitors shown in Table 1. The as prepared NiO/GNS nanocomposites exhibit specific capacitance value of 1125.8 F g⁻¹ at a current density of 2

A g^{-1} in 2 M KOH solution. This composite exhibits a good cyclic stability, with a small loss of 5.2% of maximum capacitance over a consecutive 2000 cycles.

Table 1. Electrochemical performance of NiO-based Supercapacitors.

| Specimen structure | Tested current density (A g^{-1}) | Specific capacitance (F g^{-1}) | Cycling number | Capacity retention (%) | Year Published | Ref. |
|---|--|--|----------------|------------------------|----------------|------|
| Hierarchical NiO-3D Graphene | 3 A g^{-1} | 1829 F g^{-1} | 5000 | 85% | 2014 | 21 |
| Co ₃ O ₄ /NiO core-shell nanocomposites | 2 A g^{-1} | 853 F g^{-1} | – | – | 2011 | 22 |
| 3D NF-G-NiO | 5 A g^{-1} | 950 F g^{-1} | – | – | 2016 | 23 |
| NiO/Ni/RGO core-shell | 1 A g^{-1} | 2048 F g^{-1} | 5000 | 86% | 2017 | 29 |
| CNTs/NiO | 1 A g^{-1} | 996 F g^{-1} | 10000 | 93% | 2015 | 19 |
| 3D UGF/NiO | 1 A g^{-1} | 750.8 F g^{-1} | 3000 | 100% | 2015 | 8 |
| NiO/Graphene | 2 A g^{-1} | 1125.8 F g^{-1} | 2000 | 94.8% | Present work | |

Cycling stability is an important to evaluate the electrochemical performance of supercapacitors. Liu, FG *et al.*[29] developed a novel Ni/NiO Core-shell Nanospheres for supercapacitor with 86% capacitance retention after 5000 cycles, which exhibits the excellent stability of the nickel oxide material as supercapacitor cathode.

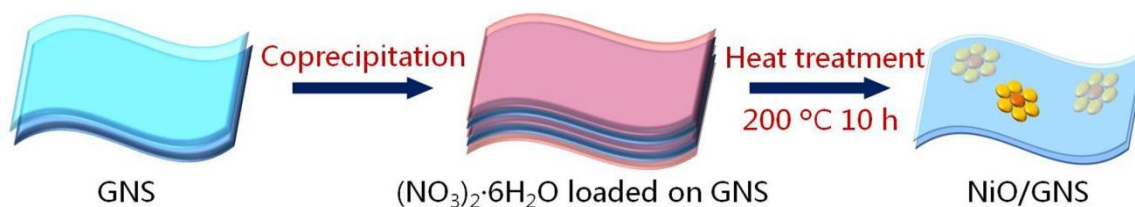


Figure 4. Schematic illustration of the NiO/GNS nanocomposite material.

As Figure 4 demonstrates, the NiO nanoparticles have a direct growth over the GNS substrate, which leads to the exposure of the NiO nanoparticles, which are well separated. This makes the nanoparticles completely accessible to the OH^- ions of the electrolyte solution while the ion diffusion is enhanced. It is guaranteed that there is strong electrical connection and mechanical adhesion between NiO nanoparticles and the conductive GNS substrate and efficient redox reactions in the process of Faradaic charge storage. It can prevent the interface resistance between active materials and binders of the conventional electrodes of the powdered materials and also the additional weight of binders. Meanwhile, the electrochemical reactions and charge transfer are accelerated by the flexible GNS which has high electrical conductivity.

4. CONCLUSIONS

To conclude, a general thermal decomposition method was used to cultivate the NiO nanoparticles over the GNS substrates. Because of the synergistic contributions made by the

pseudocapacitance-activated NiO, the highly conductive GNS, and the 3D arrays in the NiO/GNS configuration, the flexible electrode displays outstanding supercapacitor performance, these flexible NiO/GNS electrodes have a promising application into the high-performance energy storage devices. Furthermore, the strategy promoted in this paper about the electrode design can be used for the fabrication of other multifunctional hybrid electrodes for energy storage devices.

ACKNOWLEDGEMENTS

This work was supported by the National Key R&D Program of China under Grant 2017YFB0502700, the National Natural Science Foundation of China (No. 61471195), and the Fundamental Research Funds for the Central Universities (Nos. NZ2016105, NJ20150017 and NS2014040), partially by the National Defense Pre-Research Foundation of China (No.6140413020116HK02001).

References

1. S. Arico, P. Bruce, B. Scrosati, J. M. Tarascon, W. Van Schalkwijk, *Nat. Mater.*, 4 (2005) 366.
2. P. Simon, Y. Gogotsi, *Nat. Mater.*, 7 (2008) 845.
3. J. Yan, Z. Fan, W. Sun, G. Ning, T. Wei, Q. Zhang, R. Zhang, L. Zhi, F. Wei, *Adv. Funct. Mater.*, 22 (2012) 2632.
4. M. Armand, J.M. Tarascon, Building better batteries, *Nature.*, 451 (2008) 652.
5. X. Peng, L. Peng, C. Wu, Y. Xie, *Chem. Soc. Rev.*, 43 (2014) 3303.
6. S. Zheng, X. Li, B. Yan, Q. Hu, Y. Xu, X. Xiao, H. Xue, H. Pang, *Adv. Energy Mater.*, 7 (2017) 1602733.
7. J. Yu, C. Mu, B. Yan, X. Qin, C. Shen, H. Xue, H. Pang, *Mater. Horiz.*, 4 (2017) 557.
8. W. Liu, C. Lu, X. Wang, K. Tang, B.K. Tay, *J. Mater. Chem. A*, 3 (2015) 624.
9. L. Zhang, W. Zheng, H. Jiu, C. Ni, J. Chang, G. Qi, *Electrochim. Acta*, 215 (2016) 212.
10. Z. Zhang, H. Zhang, X. Zhang, D. Yu, Y. Ji, Q. Sun, Y. Wang, X. Liu, *J. Mater. Chem. A*, 4 (2016) 18578.
11. K. Chi, Z. Zhang, Q. Lv, C. Xie, J. Xiao, F. Xiao, S. Wang, *ACS Appl. Mater. Inter.*, 9 (2017) 6044.
12. S. Hu, E. L. Ribeiro, S. A. Davari, M. K. Tian, D. Mukherjee and B. Khomami *RSC Adv.*, 7 (2017) 33166.
13. Z.S. Wu, D. W. Wang, W. Ren, J. Zhao, G. Zhou, F. Li and H. M. Cheng, *Adv. Funct. Mater.*, 20 (2010) 3595.
14. W. Yao, J. Wang, H. Li and Y. Lu, *J. Power Sources*, 247 (2014) 824.
15. F. Cao, G. X. Pan, X. H. Xia, P. S. Tang and H. F. Chen, *J. Power Sources*, 264 (2014) 161.
16. M. Aghazadeh, A. Rashidi, M.R. Ganjali, M.G. Maragheh, *Int. J. Electrochem. Sci.*, 11 (2016) 11002.
17. J.L. Lv, Z.Q. Wang, H. Miura, *Solid State Commun.*, 269 (2018) 45.
18. G. Meng, Q. Yang, X. Wu, P. Wan, Y. Li, X. Sun, J. Liu, *Nano Energy*, 30 (2016) 831.
19. H. Yi, H.W. Wang, Y.T. Jing, T.Q. Peng, X.F. Wang, *J. Power Sources*, 285 (2015), 281.
20. H. Lai, Q. Wu, J. Zhao, L. Shang, H. Li, R. Che, Z. Lyu, J. Xiong, L. Yang, X. Wang, Z. Hu, *Energy Environ. Sci.*, 9 (2016) 2053.
21. C.D. Wang, J.L. Xu, M.F. Yuen, J. Zhang, Jie, Y.Y. Li, X.F. Chen, W.J. Zhang, *Adv. Funct. Mater.*, 24 (2014) 6372.
22. N.B. Trung, T.V. Tam, D.K. Dang, K.F. Babu, E.J. Kim, J. Kim, W.M. Choi, *Chem. Eng. J.*, 264 (2015) 603.
23. B. Zhao, T. Wang, L. Jiang, K. Zhang, M.M.F. Yuen, J.B. Xu, X.Z. Fu, R. Sun, C.P. Wong, *Electrochim. Acta.*, 192 (2016) 205.

24. H. Yi, H.W. Wang, Y.T. Jing, T.Q. Peng, X.F. Wang, *J. Power Sources*, 285 (2015) 281.
25. W. S. Hummers and R. E. Offeman, *J. Am. Chem. Soc.*, 80 (1958) 1339.
26. Q.L. Du, M.B. Zheng, L. F. Zhang, Y. W. Wang, J. H. Chen, L. P. Xue, W. J. Dai, G. B. Ji and J. M. Cao, *Electrochim. Acta*, 55 (2010) 3897.
27. L.S. Hu, X. Peng, Y. Li, L. Wang, K.F. Huo, L.Y.S. Lee, K.Y. Wong, P.K. Chu, *Nano Energy* 34 (2017) 515.
28. L. Zhu, W.Y. Wu, X.W. Wang, D.L. Zhu, Y.J. Shao, *Int. J. Electrochem. Sci.*, 13 (2018) 3601.
29. F.G. Liu, X.B. Wang, J. Hao, S. Han, J.S. Lian, Q. Jiang, *scientific reports*, 7 (2017) 7 17709.

© 2018 The Authors. Published by ESG (www.electrochemsci.org). This article is an open access article distributed under the terms and conditions of the Creative Commons Attribution license (<http://creativecommons.org/licenses/by/4.0/>).